Applied Mathematics and Computation 256 (2015) 131–147

Contents lists available at ScienceDirect

Applied Mathematics and Computation

journal homepage: www.elsevier.com/locate/amc

Transmission dynamics and optimal control of measles epidemics ☆

Liuyong Pang [a,c], Shigui Ruan [b,*], Sanhong Liu [a], Zhong Zhao [c], Xinan Zhang [a]

[a] School of Mathematics and Statistics, Central China Normal University, Wuhan 430079, PR China
[b] Department of Mathematics, University of Miami, Coral Gables, FL 33124-4250, USA
[c] Department of Mathematics, Huanghuai University, Zhumadian 463000, PR China

ARTICLE INFO

Keywords:
Measles
Endemic
Epidemic cycles
Vaccination strategy
Optimal control

ABSTRACT

Based on the mechanism and characteristics of measles transmission, we propose a susceptible-exposed-infectious-recovered (SEIR) measles epidemic model with vaccination and investigate the effect of vaccination in controlling the spread of measles. We obtain two critical threshold values, μ_{c1} and μ_{c2}, of the vaccine coverage ratio. Measles will be extinct when the vaccination ratio $\mu > \mu_{c1}$, endemic when $\mu_{c2} < \mu < \mu_{c1}$, and outbreak periodically when $\mu < \mu_{c2}$. In addition, we apply the optimal control theory to obtain an optimal vaccination strategy $\mu^*(t)$ and give some numerical simulations for those theoretical findings. Finally, we use our model to simulate the data of measles cases in the U.S. from 1951 to 1962 and design a control strategy.

1. Introduction

Measles is a highly contagious disease caused by the measles virus. It is spread by coughing and sneezing via close interpersonal contact or direct contact with secretions. Symptoms usually develop 10–12 days after exposure to an infectious person ([28]). There is no specific treatment for measles. Routine measles vaccination for children is the key public health strategy to prevent the disease. Today measles is still a common and often fatal disease in the world.

Data from the U.S. Centers for Disease Control and Prevention (CDC) [10] indicate that there were about 500,000 cases and 500 deaths reported annually in the U.S. before 1963, with epidemic cycles every 2–3 years. Following vaccine licensing in 1963, the incidence of measles decreased by over 98% and the 2–3-year epidemic cycles no longer occurred. But a dramatic increase in cases occurred between 1989 and 1991, during which a total of 55,622 cases was reported (18,193 in 1989; 27,786 in 1990; 9643 in 1991). In fact, the major cause of the resurgence of 1989–1991 was low vaccination coverage. In general, vaccination protects not only those who are vaccinated but also their neighbors. As a result, many others in the community can also be benefited. However, whether or not to vaccinate largely depends on the perceived risk of infection and the vaccination behavior of neighboring individuals [4,5,38]. Hence, the low risk of infection and the free-rider effects maybe be main factors which caused a low measles vaccination coverage rate before 1989. Since the measles vaccination was popularized in 1993, less than 500 cases have been reported per year and fewer than 200 cases annually since 1997. In 2004, a total of 37 cases was reported, mainly U.S. citizens traveling abroad and foreign visitors. Measles was eliminated from U.S. since 2002 (see Fig. 1(A)). In other countries, especially in developing countries, measles vaccination has not been

☆ This research was partially supported by the National Natural Science Foundation of China (Nos. 11071275, 11228104 and 11371161) and NSFC-Talent Training Fund of Henan (U1304104).

* Corresponding author.
E-mail address: ruan@math.miami.edu (S. Ruan).

http://dx.doi.org/10.1016/j.amc.2014.12.096
0096-3003/

extensively popularized. According to the report by the World Health Organization (WHO), in 2012 there were 122,000 measles deaths globally [33]. From available data reported by the Chinese Center for Disease Control and Prevention (CCDC) [11], there were 70,549 measles cases in China in 2004 and 6183 measles cases in 2012 (see Fig. 1(B)). Consequently, it is still very important to model the transmission dynamics of measles and investigate the effect of vaccination on the spread of measles.

Mathematical modeling has become an important and useful tool in studying the spread and control of infection diseases (Anderson and May [1], Zhang and Sun [35], Xia et al. [42], Diekmann and Heesterbeek [14], Zhang et al. [39], Keeling and Rohani [24], Boccaletti et al. [6], Wang and Li [31,32]). Vaccination, is one of the most effective strategies in preventing morbidity and mortality associated with various infectious diseases, has also been included in modeling. Bauch and Earn [4] investigated the impacts of vaccination policy on the level of vaccination coverage and found that voluntary vaccination was unlikely to reach the group-optimal level. Zhang et al. [37] studied the epidemic spreading with voluntary vaccination strategy on both Erdos–Renyi random graphs and Barabasi–Albert scale-free networks and Zhang et al. [36] investigated effects of behavioral response and vaccination policy on epidemic spreading. The transmission dynamics of measles epidemics have been extensively studied. In 1957, Bartlett [2] observed that the number of localized extinctions of measles was related to the population size of the community. In small communities epidemics are often followed by extinction of disease as the chain of transmission breaks down by mass vaccination (Bartlett [3], Bolker and Grenfell [9]). The critical community size above which measles can persist may depend on the spatial structure and connectedness of the regional population (Bolker and Grenfell [7,8], Keeling and Grenfell [23]). Complex dynamics such as oscillations and chaos in measles epidemic models have also attracted attentions of many researchers (Bolker and Grenfell [7], Earn et al. [16], Grenfell [19]) which are believed to be strongly related to the seasonal forcing (Conlan and Grenfell [12]). In 1960, Bartlett [3] gave an estimate of the critical community size for measles for the United States in terms of total population. Since then, various mathematical models have been developed to investigate the transmission dynamics of measles in different countries and regions (Bolker and Grenfell [9], Earn et al. [16], Ferrari et al. [17]).

Valuable information on how to more effectively prevent the outbreaks of measles and accordingly adopt appropriate vaccination policies are very important. In this article, we study the effect of vaccination by mathematical modeling and analysis and determine the level of vaccination coverage that can the most effectively prevent the spread of measles. Note that when an individual becomes infected with the measles virus, the virus begins to multiply within the cells. After an incubation period about 8 to 12 days, early measles symptoms begin. The exposed individual is not contagious during the incubation period and has life time immunity after recovery from the disease. To set up the model, we divide the total population size $N(t)$ into four distinct categories which are the susceptible, the exposed, the infectious and the recovered, with size denoted by $S(t), E(t), I(t)$ and $R(t)$ at time t, respectively. We assume that the growth of the susceptible population admits a logistic process (Kar and Batabyal [21], Wang et al. [30], Zhang and Chen [40]) in the absence of infection. The incidence rate is bilinear, i.e., proportional to the product of the number of infective individuals and the number of susceptible individuals. The model takes the following form:

$$\begin{cases} \frac{dS}{dt} = rS(1 - bS) - \beta SI - \mu S, \\ \frac{dE}{dt} = \beta SI - (d + \alpha)E, \\ \frac{dI}{dt} = \alpha E - (d + \delta)I, \\ \frac{dR}{dt} = \delta I + \mu S - dR, \end{cases} \tag{1.1}$$

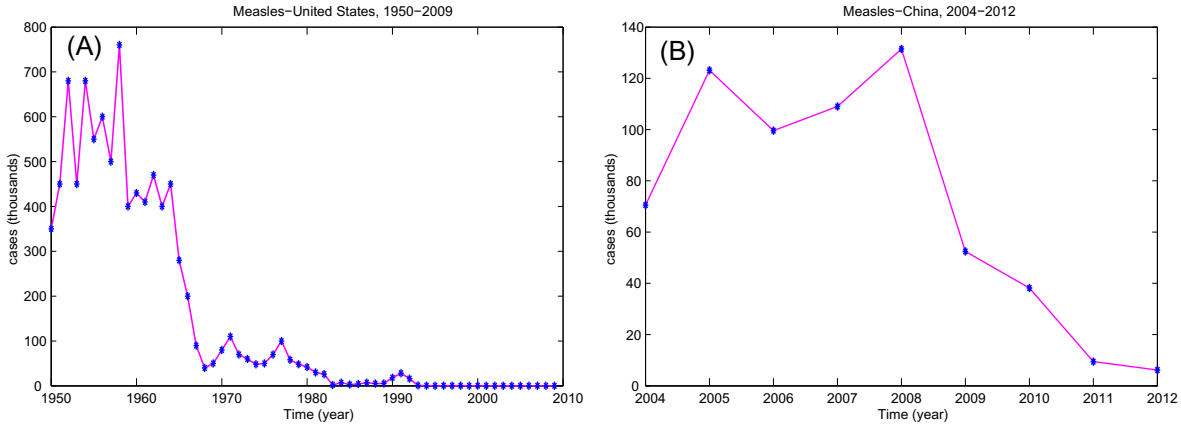

Fig. 1. Reported measles cases in the United States from 1950 to 2010 (CDC [10]) and in China from 2004 to 2012 (CCDC [11]).

where r is the intrinsic growth rate of the susceptible population, $\frac{1}{b}$ is the carrying capacity of the susceptible population in the absence of infection, β is the infective rate, μ ($\mu < r$) is the effective vaccination coverage ratio of the susceptible, d is the natural death rate, $\frac{1}{\alpha}$ is measles incubation period, δ is the recovered rate of the infective individuals.

We will study the nonlinear dynamics of the SEIR measles epidemic model (1.1) and investigate the effect of vaccination in controlling the spread of measles. We will obtain two critical threshold values μ_{c1} and μ_{c2} of vaccine coverage ratio and show that measles will be extinct when the vaccination ratio $\mu > \mu_{c1}$, will be endemic when $\mu_{c2} < \mu < \mu_{c1}$, and will be outbreak periodically when $\mu < \mu_{c2}$. In addition, we will apply the optimal control theory to obtain an optimal vaccination strategy $\mu^*(t)$ and give some numerical simulations for those theoretical findings. Finally, we will use our model to simulate the data of measles cases in the U.S. from 1951 to 1962 and give a brief discussion.

2. Basic reproduction number

Since all the parameters and state variables of model (1.1) are non-negative for $t \geqslant 0$, it is easy to show that the state variables of (1.1) remain non-negative for non-negative initial conditions. Considering the biologically feasible region

$$\Omega_1 = \left\{ (S,E,I,R) \in \mathbb{R}^4_+ : N = S + E + I + R \leqslant \frac{(r+d)^2}{4bdr} \right\},$$

we have the following conclusion.

Lemma 2.1. *The closed set Ω_1 is positively invariant for model (1.1).*

Proof. Considering a function $N = S + E + I + R$ and taking the time derivative of N along solutions of model (1.1), we have

$$\frac{dN}{dt} = \frac{dS}{dt} + \frac{dE}{dt} + \frac{dI}{dt} + \frac{dR}{dt} = rS(1 - bS) - d(E + I + R).$$

It follows that

$$\frac{dN}{dt} + dN = [r(1 - bS) + d]S \leqslant \max\{[r(1 - bS) + d]S\} = \frac{(r+d)^2}{4br}.$$

Note that $N(t) = (1 - e^{-dt})\frac{(r+d)^2}{4bdr} + N_0 e^{-dt}$ is the solution of $\frac{dN}{dt} = -dN + \frac{(r+d)^2}{4br}$ with initial value $N(0) = N_0 > 0$. Applying the well-known comparison theorem, we have

$$N(t) \leqslant (1 - e^{-dt})\frac{(r+d)^2}{4bdr} + N_0 e^{-dt},$$

which yields that $\lim_{t\to+\infty} N(t) \leqslant \frac{(r+d)^2}{4bdr}$. Thus, all solutions of model (1.1) with initial values in Ω_1 remain in the region Ω_1. Hence, the region Ω_1 is a positively invariant set of model (1.1). □

Since the first three equations in model (1.1) are independent of the variable $R(t)$, it is sufficient to consider the reduced model. Substituting $x = bS, y = bE$ and $z = \beta I$, we have the corresponding simplified model

$$\begin{cases} \frac{dx}{dt} = rx(1 - x) - xz - \mu x, \\ \frac{dy}{dt} = xz - \alpha_1 y, \\ \frac{dz}{dt} = \alpha_2 y - \alpha_3 z, \end{cases} \tag{2.1}$$

where $\alpha_1 = d + \alpha, \alpha_2 = \frac{\alpha\beta}{b}$ and $\alpha_3 = d + \delta$.

It is easy to see that model (2.1) has up to three equilibria. In fact, the trivial equilibrium $E_0(0,0,0)$ and the disease-free equilibrium $E_1(\frac{r-\mu}{r}, 0, 0)$ always exist and the endemic equilibrium $E^*(x^*, y^*, z^*)$ exists if and only if

$$\mathcal{R}_0 = \frac{r\alpha_2}{\mu\alpha_2 + r\alpha_1\alpha_3} > 1, \tag{2.2}$$

where

$$x^* = \frac{\alpha_1\alpha_3}{\alpha_2}, \quad y^* = \frac{\alpha_3(\mu\alpha_2 + r\alpha_1\alpha_3)(\mathcal{R}_0 - 1)}{\alpha_2^2}, \quad z^* = \frac{(\mu\alpha_2 + r\alpha_1\alpha_3)(\mathcal{R}_0 - 1)}{\alpha_2}.$$

$\mathcal{R}_0$ is called as the *basic reproduction number* ([15,29]) of model (2.1). The derivative of $\mathcal{R}_0$ with respect to the vaccination ratio μ is

$$\frac{d\mathcal{R}_0}{d\mu} = -\frac{r\alpha_2^2}{(\mu\alpha_2 + r\alpha_1\alpha_3)^2} < 0.$$

It follows that increasing the vaccination ratio μ can reduce the basic reproduction number $\mathcal{R}_0$. In order to facilitate the following discussion, we introduce a new quantity which is given by

$$\mathcal{R}_1 = \frac{r\alpha_2^2}{\mu\alpha_2^2 + r\alpha_1\alpha_2\alpha_3 + r(\alpha_1+\alpha_3)(\alpha_1\alpha_2+\alpha_2\alpha_3+r\alpha_1\alpha_2\alpha_3)}. \tag{2.3}$$

It is easy to see that $\mathcal{R}_0 > \mathcal{R}_1$.

3. Stability of the equilibria

In this section, sufficient conditions for the asymptotic stability of the equilibria will be derived.

Lemma 3.1. *The trivial equilibrium E_0 is a saddle which is unstable.*

To obtain the stability of the disease-free equilibrium E_1, we present the following lemma.

Lemma 3.2. *$\Omega_2 = \{(x,y,z) \in \mathbb{R}^3_+ : x \leqslant \frac{r-\mu}{r}\}$ is a positively invariant set for model (2.1).*

Proof. It follows from the first equation of model (2.1) that

$$\frac{dx}{dt} = rx(1-x) - xz - \mu x = (r-\mu)x - rx^2 - xz \leqslant (r-\mu)x\left[1 - \frac{x}{\frac{r-\mu}{r}}\right].$$

Note that $x(t) = \frac{\frac{r-\mu}{r}x_0}{x_0 - \left[x_0 - \frac{r-\mu}{r}\right]e^{-(r-\mu)t}}$ is the solution of $\frac{dx}{dt} = (r-\mu)x\left[1 - \frac{x}{\frac{r-\mu}{r}}\right]$ with initial value $x(0) = x_0 > 0$. By the comparison theorem, we have

$$x(t) \leqslant \frac{\frac{r-\mu}{r}x_0}{x_0 - [x_0 - \frac{r-\mu}{r}]e^{-(r-\mu)t}},$$

which yields that $\lim_{t\to\infty} x(t) \leqslant \frac{r-\mu}{r}$. Thus, all solutions of model (2.1) with initial values in Ω_2 remain in the region Ω_2. That is, the region Ω_2 is a positively invariant set of model (2.1). □

Theorem 3.3. *The disease-free equilibrium E_1 is globally asymptotically stable in the set Ω_2 if $\mathcal{R}_0 < 1$ and unstable if $\mathcal{R}_0 > 1$.*

Proof. The characteristic equation of model (2.1) at E_1 is given by

$$[\lambda + (r-\mu)]\left[(\lambda+\alpha_3)(\lambda+\alpha_1) - \alpha_2\frac{r-\mu}{r}\right] = 0.$$

One eigenvalue is $\lambda_1 = -(r-\mu) < 0$ and the other two eigenvalues are determined by

$$(\lambda+\alpha_3)(\lambda+\alpha_1) - \alpha_2\frac{r-\mu}{r} = \lambda^2 + (\alpha_1+\alpha_3)\lambda + \alpha_1\alpha_3 - \alpha_2\frac{r-\mu}{r} = 0.$$

Clearly, $\alpha_1+\alpha_3 > 0$ and $\alpha_1\alpha_3 - \alpha_2\frac{r-\mu}{r} = \frac{(\alpha_2\mu + r\alpha_1\alpha_3)(1-\mathcal{R}_0)}{r} > 0$ provided that $\mathcal{R}_0 < 1$. Therefore, the disease-free equilibrium E_1 is locally asymptotically stable if $\mathcal{R}_0 < 1$ and unstable if $\mathcal{R}_0 > 1$.

To discuss the global stability of E_1, we use a Lyapunov function

$$W = \alpha_2 y + \alpha_1 z.$$

The derivative of W along solutions of model (2.1) is calculated as follows

$$\frac{dW}{dt} = \alpha_2\frac{dy}{dt} + \alpha_1\frac{dz}{dt} = z(\alpha_2 x - \alpha_1\alpha_3) \leqslant z\left(\alpha_2\frac{r-\mu}{r} - \alpha_1\alpha_3\right) = z\frac{(\alpha_2\mu + \alpha_1\alpha_3 r)(\mathcal{R}_0 - 1)}{r}.$$

Then $\frac{dW}{dt} < 0$ when $\mathcal{R}_0 < 1$, which indicates that E_1 is globally asymptotically stable if $\mathcal{R}_0 < 1$. □

Theorem 3.4. *The unique endemic equilibrium E^* is locally asymptotically stable if $\mathcal{R}_1 < 1 < \mathcal{R}_0$ and unstable if $\mathcal{R}_1 > 1$.*

Proof. The Jacobian matrix at E^* of model (2.1) is

$$J(E^*) = \begin{bmatrix} -rx^* & 0 & -x^* \\ z^* & -\alpha_1 & x^* \\ 0 & \alpha_2 & -\alpha_3 \end{bmatrix}.$$

The characteristic equation of $J(E^*)$ is given by

$$f(\lambda) = \lambda^3 + A_1\lambda^2 + A_2\lambda + A_3 = 0, \tag{3.1}$$

where

$$A_1 = \alpha_1 + \alpha_3 + rx^* > 0,$$

$$A_2 = (\alpha_1\alpha_3 - \alpha_2 x^*) + rx^*(\alpha_1 + \alpha_3) = rx^*(\alpha_1 + \alpha_3) > 0,$$

$$A_3 = rx^*(\alpha_1\alpha_3 - \alpha_2 x^*) + \alpha_2 x^* z^* = \alpha_2 x^* z^* > 0,$$

$$\begin{aligned} A_1A_2 - A_3 &= (\alpha_1 + \alpha_3 + rx^*)rx^*(\alpha_1 + \alpha_3) - \alpha_2 x^* z^* = x^*[r(\alpha_1 + \alpha_3 + rx^*)(\alpha_1 + \alpha_3) - r\alpha_2 + \mu\alpha_2 + r\alpha_1\alpha_3] \\ &= x^*[r(\alpha_1 + \alpha_3 + rx^*)(\alpha_1 + \alpha_3) + \mu\alpha_2 + r\alpha_1\alpha_3](1 - \mathcal{R}_1). \end{aligned}$$

It is obvious that $A_1A_2 - A_3 > 0$ when $\mathcal{R}_1 < 1$, and $A_1A_2 - A_3 < 0$ when $\mathcal{R}_1 > 1$. Hence, if $\mathcal{R}_1 < 1 < \mathcal{R}_0$, the endemic equilibrium E^* is locally asymptotically stable. If $\mathcal{R}_1 > 1$, the endemic equilibrium E^* is unstable. □

4. Hopf bifurcation at the endemic equilibrium

From Theorem 3.4, we know that if $\mathcal{R}_1 = 1$, i.e., $A_1A_2 - A_3 = 0$, J has one negative eigenvalue $\lambda = -A_1$ and two purely imaginary eigenvalues $\lambda_{2,3} = \pm\omega i$ (where $\omega = \sqrt{A_2} > 0$), which suggests that model (2.1) may have a Hopf bifurcation when $\mathcal{R}_1 = 1$. We explore the existence of the Hopf bifurcation. First of all, we quote a useful lemma.

Lemma 4.1 ([34,27]). *Let $\Omega \in \mathbb{R}^3$ be an open set containing $O(x_1, x_2, x_3)$ and let $S \subseteq \mathbb{R}$ be an open set with $0 \in S$. Let $f : \Omega \times S \to \mathbb{R}^3$ be an analytic function such that $f(0, \rho) = 0$ for any $\rho \in S$. Assume that the variational matrix $Df(0, \rho)$ of f has one real eigenvalue $\gamma(\rho)$ and two conjugate imaginary eigenvalues $\alpha(\rho) \pm i\beta(\rho)$ with $\gamma(0) < 0, \alpha(0) = 0, \beta(0) > 0$. Furthermore, suppose that the eigenvalues cross the imaginary axis with nonzero speed, that is, $\frac{d\alpha(0)}{d\rho} \neq 0$. Then the following differential system*

$$\dot{X} = f(X, \rho)$$

undergoes a Hopf bifurcation near the equilibrium point O at $\rho = 0$.

Here we choose the intrinsic growth rate r as the perturbation parameter. By Theorem 3.4, we can see that

$$\begin{aligned} A_1A_2 - A_3 &= x^*[r(\alpha_1 + \alpha_3 + rx^*)(\alpha_1 + \alpha_3) - r\alpha_2 + \mu\alpha_2 + r\alpha_1\alpha_3] = x^*\{[r(\alpha_1 + \alpha_3) + r^2x^*](\alpha_1 + \alpha_3) - r\alpha_2 + r\alpha_1\alpha_3 + \mu\alpha_2\} \\ &= x^*\left\{x^*(\alpha_1 + \alpha_3)r^2 + [(\alpha_1 + \alpha_3)^2 + \alpha_1\alpha_3 - \alpha_2]r + \mu\alpha_2\right\} = x^*f(r). \end{aligned}$$

Thus, the equation $A_1A_2 - A_3 = 0$ is equivalent to the following quadratic equation

$$f(r) = x^*(\alpha_1 + \alpha_3)r^2 + [(\alpha_1 + \alpha_3)^2 + \alpha_1\alpha_3 - \alpha_2]r + \mu\alpha_2 = 0, \tag{4.1}$$

and also implies that $\mathcal{R}_1 = 1$. $\mathcal{R}_1 = 1$ is, in turn, equivalent to

$$\begin{aligned} r\alpha_2 &= \mu\alpha_2 + r\alpha_1\alpha_3 + r(\alpha_1 + \alpha_3)(\alpha_1 + \alpha_3 + rx^*) = r\alpha_1\alpha_3 + r(\alpha_1 + \alpha_3)^2 + \mu\alpha_2 + r^2(\alpha_1 + \alpha_3)x^* \\ &\geqslant r\alpha_1\alpha_3 + r(\alpha_1 + \alpha_3)^2 + 2r\sqrt{\mu\alpha_2 x^*(\alpha_1 + \alpha_3)}. \end{aligned}$$

This shows that

$$\alpha_2 \geqslant \alpha_1\alpha_3 + (\alpha_1 + \alpha_3)^2 + 2\sqrt{\mu\alpha_2 x^*(\alpha_1 + \alpha_3)}$$

always holds if $\mathcal{R}_1 = 1$. Hence, the corresponding discriminant of the quadratic function of Eq. (4.1) satisfies

$$\begin{aligned} \Delta &= \left[\alpha_2 - \alpha_1\alpha_3 - (\alpha_1 + \alpha_3)^2\right]^2 - 4\mu\alpha_2 x^*(\alpha_1 + \alpha_3) \\ &= \left[\alpha_2 - \alpha_1\alpha_3 - (\alpha_1 + \alpha_3)^2 + 2\sqrt{\mu\alpha_2 x^*(\alpha_1 + \alpha_3)}\right]\left[\alpha_2 - \alpha_1\alpha_3 - (\alpha_1 + \alpha_3)^2 - 2\sqrt{\mu\alpha_2 x^*(\alpha_1 + \alpha_3)}\right] \geqslant 0. \end{aligned}$$

Therefore, there exist two positive real roots (see Fig. 2(a))

$$r_{c1} = \frac{\alpha_2 - \alpha_1\alpha_3 - (\alpha_1 + \alpha_3)^2 - \sqrt{[(\alpha_1 + \alpha_3)^2 + \alpha_1\alpha_3 - \alpha_2]^2 - 4\mu\alpha_2(\alpha_1 + \alpha_3)x^*}}{2x^*(\alpha_1 + \alpha_3)},$$

$$r_{c2} = \frac{\alpha_2 - \alpha_1\alpha_3 - (\alpha_1 + \alpha_3)^2 + \sqrt{[(\alpha_1 + \alpha_3)^2 + \alpha_1\alpha_3 - \alpha_2]^2 - 4\mu\alpha_2(\alpha_1 + \alpha_3)x^*}}{2x^*(\alpha_1 + \alpha_3)},$$

and when $\Delta = 0$ there exists one positive real root with multiplicity two (see Fig. 2(b))

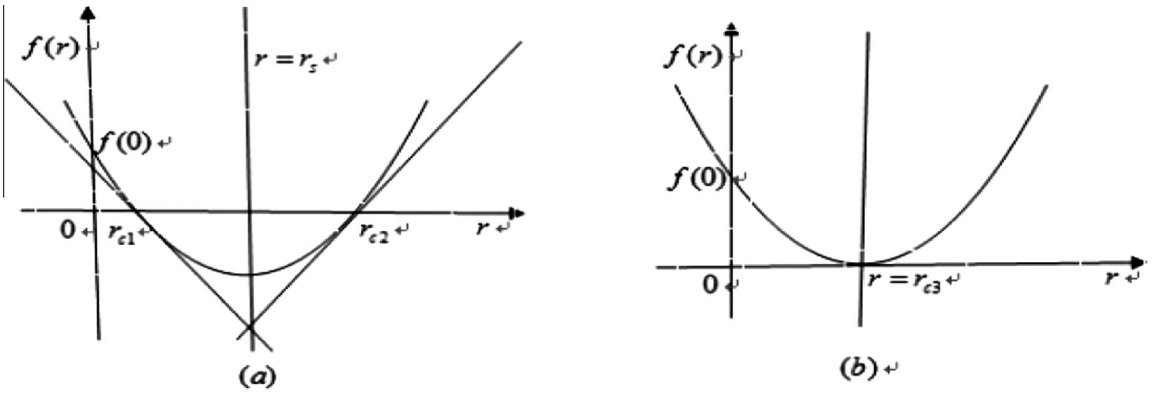

Fig. 2. (a) The graph of $f(r)$ when $\Delta > 0$ and (b) The graph of $f(r)$ when $\Delta = 0$.

$$r_{c3} = \frac{\alpha_2 - \alpha_1\alpha_3 - (\alpha_1+\alpha_3)^2}{2x^*(\alpha_1+\alpha_3)}.$$

To sum up, if $\mu < r < r_{c1}$ or $r > r_{c2}$, then $f(r) > 0$ (i.e., $A_1A_2 - A_3 > 0$), which indicates that the endemic equilibrium E^* is locally asymptotically stable. While if $r_{c1} < r < r_{c2}$, then $f(r) < 0$ (i.e., $A_1A_2 - A_3 < 0$), which implies that E^* is unstable and periodic solutions may arise from the endemic equilibrium via Hopf bifurcation.

Without loss of generality, we set $r_i(\rho) = r_{ci} + \rho$ $(i = 1, 2, 3)$, where $r_i(0) = r_{ci}$ satisfies that

$$(A_1A_2 - A_3)|_{r_i(0)=r_{ci}} = 0. \tag{4.2}$$

We also need to determine the sign of the real part of $\frac{d\lambda}{d\rho}$ at $\rho = 0$ when the above equation is valid. Differentiating Eq. (3.1) with respect to ρ, we have

$$3\lambda^2\frac{d\lambda}{d\rho} + x^*\lambda^2 + 2A_1\lambda\frac{d\lambda}{d\rho} + x^*(\alpha_1+\alpha_3)\lambda + A_2\frac{d\lambda}{d\rho} + (\alpha_2 - \alpha_1\alpha_3)x^* = 0,$$

which leads to

$$\frac{d\lambda}{d\rho} = -\frac{x^*\lambda^2 + x^*(\alpha_1+\alpha_3)\lambda + (\alpha_2 - \alpha_1\alpha_3)x^*}{3\lambda^2 + 2A_1\lambda + A_2}. \tag{4.3}$$

Thus

$$\begin{aligned}
V_c &= \operatorname{sign}\left\{\operatorname{Re}\left(\frac{d\lambda}{d\rho}\Big|_{\rho=0}\right)\right\} = \operatorname{sign}\left\{\operatorname{Re}\left(-\frac{-\omega^2x^* + x^*(\alpha_1+\alpha_3)\omega i + (\alpha_2 - \alpha_1\alpha_3)x^*}{-3\omega^2 + 2A_1\omega i + A_2}\right)\right\} \\
&= \operatorname{sign}\left\{\operatorname{Re}\left(\frac{\alpha_2 - \alpha_1\alpha_3 - A_2 + (\alpha_1+\alpha_3)\omega i}{A_2 - A_1\omega i}\right)\right\} = \operatorname{sign}\{\alpha_2 - \alpha_1\alpha_3 - A_2 + (\alpha_1+\alpha_3)A_1\} \\
&= \operatorname{sign}\{\alpha_2 - \alpha_1\alpha_3 - rx^*(\alpha_1+\alpha_3) + (\alpha_1+\alpha_3)(\alpha_1+\alpha_3+rx^*)\} = \operatorname{sign}\left\{\alpha_2 - \alpha_1\alpha_3 - (\alpha_1+\alpha_3)^2 - 2rx^*(\alpha_1+\alpha_3)\right\} \\
&= \operatorname{sign}\left\{-\frac{df(r)}{dr}\right\}.
\end{aligned}$$

From Fig. 2, we know that $V_{c1} = 1 \neq 0$ if $r = r_{c1}, V_{c2} = -1 \neq 0$ if $r = r_{c2}$ and $V_{c3} = 0$ if $r = r_{c3}$. Hence, we have the following result.

Theorem 4.2. *If $r = r_{c1}$ or $r = r_{c2}$, then model (2.1) undergoes a non-degenerate Hopf bifurcation at the endemic equilibrium E^*.*

Note that if $r = r_{c3}$, then the real part of $\frac{d\lambda}{d\rho}|_{\rho=0}$ becomes zero such that the transversality condition fails. To determine the whether or not a degenerate Hopf bifurcation occurs, differentiate (4.3) again with respect to ρ, we obtain that

$$\begin{aligned}
\frac{d^2\lambda}{d\rho^2} = &-\frac{[2x^*\lambda + x^*(\alpha_1+\alpha_3)](3\lambda^2 + 2A_1\lambda + A_2)\frac{d\lambda}{d\rho}}{(3\lambda^2 + 2A_1\lambda + A_2)^2} \\
&+ \frac{\left[(6\lambda + 2A_1)\frac{d\lambda}{d\rho} + 2\lambda x^* + x^*(\alpha_1+\alpha_3)\right]\left[x^*\lambda^2 + x^*(\alpha_1+\alpha_3)\lambda + (\alpha_2 - \alpha_1\alpha_3)x^*\right]}{(3\lambda^2 + 2A_1\lambda + A_2)^2}.
\end{aligned}$$

It follows from the assumption (4.2) and the fact $\alpha_2 = \alpha_{22}^*$ that $\mathrm{Re}(\frac{d\lambda}{d\rho}|_{\rho=0}) = 0$, which implies that $\alpha_2 = \alpha_1\alpha_3 + (\alpha_1+\alpha_3)^2 + 2r_{c3}(\alpha_1+\alpha_3)x^*$ holds. Then

$$\begin{aligned}
\mathrm{sign}\left\{\mathrm{Re}\left(\frac{d^2\lambda}{d\rho^2}\Big|_{\rho=0}\right)\right\} &= \mathrm{sign}\left\{\mathrm{Re}\left(\frac{(2\omega i+\alpha_1+\alpha_3)[-A_2+(\alpha_1+\alpha_3)\omega i+(\alpha_2-\alpha_1\alpha_3)]}{(-3A_2^2+2A_1\omega i+A_2)^2}\right)\right\}\\
&= \mathrm{sign}\left\{\mathrm{Re}\left(\frac{(\alpha_1+\alpha_3)(\alpha_2-\alpha_1\alpha_3-A_2)-2(\alpha_1+\alpha_3)A_2+[2(\alpha_2-\alpha_1\alpha_3-A_2)+(\alpha_1+\alpha_3)^2]\omega i}{(A_2-A_1\omega i)^2}\right)\right\}\\
&= \mathrm{sign}\left\{[(\alpha_1+\alpha_3)^2A_1-2(\alpha_1+\alpha_3)A2](A_2-A_1^2)-2A_1A_2[2(\alpha_1+\alpha_3)A_1+(\alpha_1+\alpha_3)^2]\right\}\\
&= \mathrm{sign}\left\{[(\alpha_1+\alpha_3)A_1-2A_2](A_2-A_1^2)-2A_1A_2[2A_1+(\alpha_1+\alpha_3)]\right\}\\
&= \mathrm{sign}\left\{(\alpha_1+\alpha_3)A_1A_2-(\alpha_1+\alpha_3)A_1^3-2A_2^2+2A_2A_1^2-4A_1^2A_2-2(\alpha_1+\alpha_3)A_1A_2\right\}\\
&= \mathrm{sign}\left\{-(\alpha_1+\alpha_3)(A_1A_2+A_1^3)-2A_2(A_2+A_1^2)\right\} = -1 < 0.
\end{aligned}$$

Hence, if $r = r_{c3}$, then $\mathrm{Re}(\frac{d\lambda}{d\rho}|_{\rho=0}) = 0$ and $\mathrm{Re}(\frac{d^2\lambda}{d\rho^2}|_{\rho=0}) < 0$. That is, $\rho = 0$ is local maximum point of the real part of eigenvalues (i.e., $\alpha(\rho) < \alpha(0) = 0$ is always satisfied when $0 < |\rho| \ll 1$). It indicates that the endemic equilibrium E^* is locally asymptotically stable when $r = r_{c3}$. So we obtain the following theorem.

Theorem 4.3. *If $\Delta = 0$, there is no Hopf bifurcation for model (2.1) at the endemic equilibrium E^*.*

Remark 4.4. From the above theoretical analyses, we have obtained the following results. If

$$\mu > \frac{r\alpha_2 - r\alpha_1\alpha_3}{\alpha_2} \triangleq \mu_{c1},$$

i.e., $\mathcal{R}_0 < 1$, measles will be extinct eventually. If

$$\mu_2 \triangleq \frac{r\alpha_2 - r\alpha_1\alpha_3 - r(\alpha_1+\alpha_3)(\alpha_1+\alpha_2\alpha_1)}{\alpha_2} < \mu < \mu_{c1},$$

i.e., $\mathcal{R}_1 < 1 < \mathcal{R}_0$, measles will be endemic. If $\mu < \mu_{c2}$ (i.e., $\mathcal{R}_1 > 1$), then measles will be outbreak periodically. The outbreaks of measles in the United States before 1963 were about 2–3 years (see Fig. 7).

To investigate the stability of the periodic solutions generated from the Hopf bifurcation of the 3-dimensional model (2.1), we need to use the center manifold theorem, the normal form theory, and the criterion for super- or sub-critical Hopf bifurcation in the 2-dimensional space. The stability of the periodic solution and the direction of bifurcation depend on the sign of the value of a stability quantity K at the bifurcation point. Details for the stability quantity K are given in Appendix A. Although we have not been able to obtain a simple express of K to find general conditions for stability, our results can be used to calculate the stability quantity K numerically.

5. Optimal vaccination strategy

Optimal control theory has been used to explore optimal control strategies for various infectious diseases, see, for example, Kirschner et al. [25], Culshaw et al. [13], Karrakchou et al. [22], Kar and Batabyal [21], Lenhart and Workman [26], and the references cited therein. The objective of this section is to seek an optimal vaccination strategy to prevent the spread of measles. Specifically, the optimal vaccination strategy aims at exploring the possibility of achieving the following two goals:

(1) To make the number of infectious individuals $z(t)$ as small as possible during a certain vaccination period.
(2) To keep the vaccination ratio of measles as low as possible during a certain vaccination period.

The vaccination ratio $\mu(t)$ is not more than the intrinsic growth rate r of the susceptible, that is, $\mu(t) \in [0, r]$. For these reasons, we use optimal control techniques to study the optimal vaccination rate of susceptible individuals. The vaccination rate is chosen as a control variable and we consider the following objective functional associated with model (2.1):

$$\min J(\mu) = \min_{0\leqslant\mu(t)\leqslant r} \int_0^T [z(t) + \frac{\tau}{2}\mu^2(t)]dt \tag{5.1}$$

in $\Omega_3 = \{\mu(t) \in L^1(0,T) | 0 \leqslant \mu(t) \leqslant r\}$, where T represents the vaccination period, τ denotes a positive weight parameter. Model (2.1) can be written as

$$\phi_t = \begin{bmatrix} \dot{x} \\ \dot{y} \\ \dot{z} \end{bmatrix} = g(t,\phi,\mu) = \begin{bmatrix} rx(1-x) - xz - \mu x \\ xz - \alpha_1 y \\ \alpha_2 y - \alpha_3 z \end{bmatrix}.$$

We have the existence of an optimal vaccination strategy.

Theorem 5.1. *For the objective functional $J(\mu)$ associated with model (2.1) defined in Ω_3, there exists an optimal vaccination strategy μ^* minimizing $J(\mu)$.*

Proof. To prove the existence of an optimal vaccination strategy μ^* minimizing $J(\mu)$, we apply Theorem III.4.1 from [18], that is, we only need to check the following assumptions:

(H1) The set of controls and corresponding state variables is non-empty.
(H2) The admissible control set is convex and closed.
(H3) Each right hand side of the state system is continuous, is bounded above by a sum of the bounded control and the state, and can be written as a linear function of μ with coefficients depending on time and the state.
(H4) The integrand of the objective functional is concave.
(H5) There exist constants $C_1, C_2 > 0$, and $\beta^* > 1$ such that the integrand of the objective functional satisfies $L(t,\phi,\mu) \geqslant C_1|\mu|^{\beta^*} - C_2$.

It is obvious that Ω_3 is an nonempty set of Lebesgue integrable functions on $0 \leqslant t \leqslant T$ with values in $\mathbb{R}$. Note that the solutions are bounded, so the admissible control set is bounded and convex. For the assumption (H3), it follows that

$$\begin{aligned}
|g(t,\phi_1,\mu) - g(t,\phi_2,\mu)| &= \left| \begin{bmatrix} rx_1(1-x_1) - x_1Z_1 - \mu x_1 - rx_2(1-x_2) + x_2z_2 + \mu x_2 \\ x_1z_1 - \alpha_1 y_1 - x_2z_2 + \alpha_1 y_2 \\ \alpha_2 y_1 - \alpha_3 z_1 - \alpha_2 y_2 + \alpha_3 z_2 \end{bmatrix} \right| \\
&= \left| \begin{bmatrix} (r-\mu)(x_1-x_2) + r(x_2+x_1)(x_2-x_1) + x_2(z_2-z_1) + z_1(x_2-x_1) \\ x_2(z_1-z_2) + z_1(x_1-x_2) + \alpha_1(y_2-y_1) \\ \alpha_2(y_1-y_2) + \alpha_3(z_2-z_1) \end{bmatrix} \right| \\
&\leqslant (r-\mu)|x_1-x_2| + r|x_2+x_1||x_1-x_2| + |x_2||z_2-z_1| + |z_1||x_2-x_1| \\
&\quad + |x_2||z_1-z_2| + |z_1||x_1-x_2| + \alpha_1|y_2-y_1| + \alpha_2|y_1-y_2| + \alpha_3|z_2-z_1| \\
&= \{(r-\mu) + r|x_2+x_1| + 2|z_1|\}|x_2-x_1| + (\alpha_1+\alpha_2)|y_2-y_1| + (2|x_2|+\alpha_3)|z_2-z_1| \\
&\leqslant M_1|x_2-x_1| + M_2|y_2-y_1| + M_3|z_2-z_1| \leqslant M(|x_2-x_1| + |y_2-y_1| + |z_2-z_1|) = M|\phi_1-\phi_2|,
\end{aligned}$$

where $M_1 = (r-\mu) + \frac{(r+d)^2(rb+\beta)}{2bdr}, M_2 = \alpha_1+\alpha_2, M_3 = \alpha_3 + \frac{(r+d)^2}{2dr}$ and $M = \max\{M_1, M_2, M_3\}$. Thus, assumption (H3) is also satisfied.

Let $p \in (0,1)$ and $u(t), v(t) \in \Omega_3$, we have

$$\begin{aligned}
L(t,z(t),(1-p)u(t)+pv(t)) - (1-p)L(t,z(t),u(t)) - pL(t,z(t),v(t)) &= \frac{\tau}{2}\left[(1-p)^2u^2(t) + p^2v^2(t) + 2p(1-p)u(t)v(t)\right] \\
&\quad - \frac{\tau}{2}u^2(t) - \frac{\tau}{2}v^2(t) = \frac{\tau}{2}(p^2-p)(u(t) \\
&\quad - v(t))^2 < 0 \Leftarrow p \in (0,1), \quad p^2 < p.
\end{aligned}$$

Hence, $L(t,z(t),(1-p)u(t)+pv(t)) < (1-p)L(t,z(t),u(t)) + pL(t,z(t),v(t))$, which shows that the assumption (H4) holds.

Finally, notice that

$$z(t) + \frac{\tau}{2}\mu^2(t) \geqslant \frac{\tau}{2}\mu^2(t) \geqslant C_1|\mu|^{\beta^*} - C_2$$

with $C_1 = \frac{\tau}{2}, \beta^* = 2$, and $C_2 > 0$. So assumption $(H5)$ is satisfied. Hence, there exists an optimal vaccination strategy μ^* minimizing $J(\mu)$. □

We now seek for the minimal value of $J(\mu)$. To accomplish this, we define the Hamiltonian H for the control problem as

$$H(t,\phi(t),\mu(t)) = z(t) + \frac{\tau}{2}\mu^2(t) + \sum_{i=1}^{3}\lambda_i g_i(t,\phi,\mu). \tag{5.2}$$

If $(\phi^*(t),\mu^*(t))$ is an optimal solution of the optimal control problem, then there exists a non-trivial vector function $\lambda(t) = (\lambda_1(t),\lambda_2(t),\lambda_3(t))$ satisfying the following equalities:

$$\begin{cases} \frac{d\phi(t)}{dt} = \frac{\partial H(t,\phi(t),\mu^*(t),\lambda(t))}{\partial \lambda}, \\ 0 = \frac{\partial H(t,\phi(t),\mu^*(t),\lambda(t))}{\partial \mu}, \\ \lambda'(t) = -\frac{\partial H(t,\phi(t),\mu^*(t),\lambda(t))}{\partial \phi}. \end{cases}$$

It follows from the above derivative that

$$\begin{cases} \mu^*(t) = 0, & \text{if } \frac{\partial H}{\partial \mu} < 0, \\ 0 \leqslant \mu^*(t) \leqslant r, & \text{if } \frac{\partial H}{\partial \mu} = 0, \\ \mu^*(t) = r, & \text{if } \frac{\partial H}{\partial \mu} > 0. \end{cases}$$

Now, we apply the necessary conditions to the Hamiltonian H given by (5.2). Following the results in ([26]), we have the following conclusions.

Theorem 5.2. *Let $(x^*(t), y^*(t), z^*(t))$ be an optimal orbit associated with the optimal vaccination strategy $\mu^*(t)$ for the optimal control problem (5.1), then there exist adjoint variables $\lambda_1(t), \lambda_2(t)$ and $\lambda_3(t)$ that satisfy*

$$\begin{cases} \dot{\lambda_1} = -\lambda_1(r - \mu - 2rx^*(t) - z) - \lambda_2 z^*(t), \\ \dot{\lambda_2} = \lambda_2\alpha_1 - \lambda_3\alpha_2, \\ \dot{\lambda_3} = -1 + (\lambda_1 - \lambda_2)x^*(t) + \lambda_3\alpha_3 \end{cases}$$

with the boundary conditions $\lambda_i(T) = 0 (i = 1, 2, 3)$. Moreover, the optimal vaccination strategy $\mu^*(t)$ is given by $\mu^*(t) = \min\{r, \max\{0, \frac{\lambda_1 x^*(t)}{\tau}\}\}$.

Proof. To determine the adjoin equations and the boundary conditions, we use the Hamiltonian (5.2). Setting $x(t) = x^*(t), y(t) = y^*(t)$ and $z(t) = z^*(t)$, and differentiating the Hamiltonian (5.2) with respect to x, y and z, we have

$$\dot{\lambda_1} = -\frac{\partial H}{\partial x} = -\lambda_1(r - \mu - 2rx^*(t) - z) - \lambda_2 z^*(t),$$

$$\dot{\lambda_2} = -\frac{\partial H}{\partial y} = \lambda_2\alpha_1 - \lambda_3\alpha_2,$$

$$\dot{\lambda_3} = -\frac{\partial H}{\partial z} = -1 + (\lambda_1 - \lambda_2)x^*(t) + \lambda_3\alpha_3.$$

By the optimality condition, we obtain that

$$\frac{\partial H}{\partial \mu^*} = \tau\mu^*(t) - \lambda_1 x^*(t) = 0, \quad \Rightarrow \mu^*(t) = \frac{\lambda_1 x^*(t)}{\tau}.$$

Using the property of the control space, we have

$$\begin{cases} \mu^*(t) = 0, & \text{if } \frac{\lambda_1 x^*(t)}{\tau} < 0, \\ 0 \leqslant \mu^*(t) \leqslant r, & \text{if } \frac{\lambda_1 x^*(t)}{\tau} = 0, \\ \mu^*(t) = r, & \text{if } \frac{\lambda_1 x^*(t)}{\tau} > 0. \end{cases}$$

This can be rewritten in compact notation

$$\mu^*(t) = \min\left\{r, \max\left\{0, \frac{\lambda_1 x^*(t)}{\tau}\right\}\right\}. \tag{5.3}$$

This proves the conclusions. □

To solve the optimality system, we use the initial and boundary conditions together with the characterization of the optimal control $\mu^*(t)$ given by (5.3). In addition, the second derivative of the Lagrangian with respect to μ is positive, which shows that the optimal problem is minimum at control $\mu^*(t)$. By substituting the values of $\mu^*(t)$ in the control model (5.1), we get the following model

$$\begin{cases} \frac{dx^*}{dt} = rx^*(t)(1 - x^*(t)) - x^*(t)z^*(t) - \min\{r, \max\{0, \frac{\lambda_1 x^*(t)}{\tau}\}\}x^*(t), \\ \frac{dy^*}{dt} = x^*(t)z^*(t) - \alpha_1 y^*(t), \\ \frac{dz^*}{dt} = \alpha_2 y^*(t) - \alpha_3 z^*(t), \end{cases}$$

To find out the optimal control and states, we will numerically solve the above model.

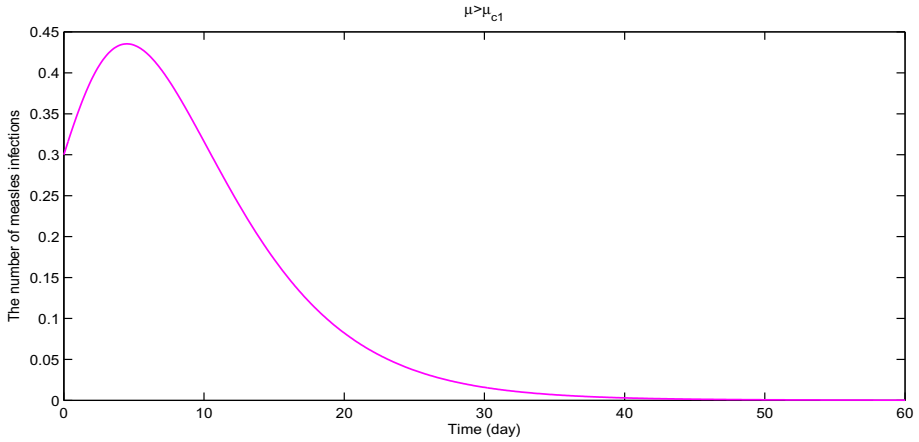

Fig. 3. The plot represents the variation of the number of infectious individuals $I(t)$ with time when $\mu = 0.7033$ ($\mu > \mu_{c1}$).

6. Numerical simulations

From Remark 4.4, we know that the measles-free equilibrium is globally asymptotically stable if the vaccination ratio of susceptible population $\mu > \mu_{c1}$, the endemic equilibrium is asymptotically stable if $\mu_{c2} < \mu < \mu_{c1}$, and measles appears in epidemic cycles if $\mu < \mu_{c2}$. Hence, we choose some suitable parameters of model (2.1) to simulate the theoretical conclusions obtained in the previous sections.

Choosing the following parameters values $r = 0.8, \alpha_1 = 0.22, \alpha_2 = 0.4$ and $\alpha_3 = 0.22$, we obtain that $\mu_{c1} = 0.7032$ and $\mu_{c2} = 0.2308$.

Case 1: $\mu > \mu_{c1}$
When $\mu = 0.7033$, measles will become extinct ultimately (see Fig. 3).

Case 2: $\mu_{c2} < \mu < \mu_{c1}$
When $\mu = 0.4$, measles will become endemic as shown in Fig. 4 which shows that the number of the infectious individuals will be in a stable level.

Case 3: $\mu < \mu_{c2}$
When $\mu = 0.2$, measles will be outbreak periodically (see Fig. 5).

Case 4: The optimal vaccination strategy $\mu^*(t)$
To control the spread of measles at the lowest economical cost, we apply optimal control theory to obtain the optimal vaccination strategy $\mu^*(t)$ by numerical calculations. We take $\tau = 0.001$ and the remaining parameters as same as above. The changes of the infectious individuals and corresponding optimal vaccination strategy $\mu^*(t)$ with time are shown in Fig. 6. To prevent the spread of measles more effectively, we should adopt the large vaccination ratio at the beginning and reduce vaccination ratio gradually (see Fig. 6(B)).

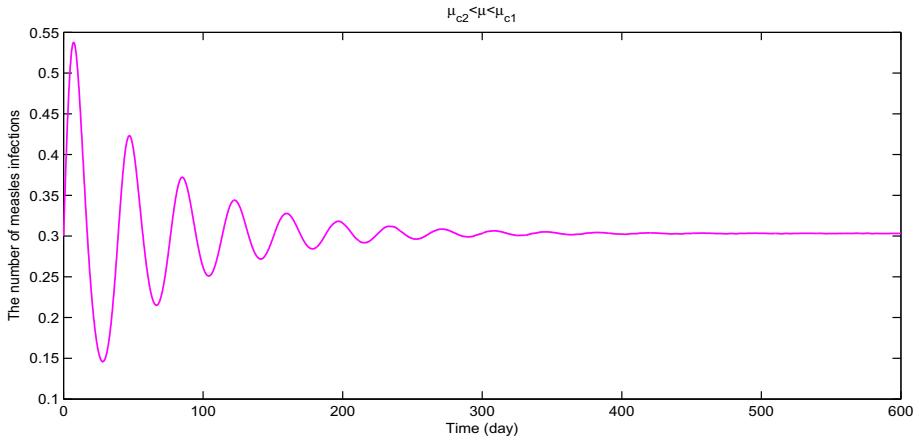

Fig. 4. The plot represents the variation of the number of infectious individuals $I(t)$ with time when $\mu = 0.4$ ($\mu_{c2} < \mu < \mu_{c1}$).

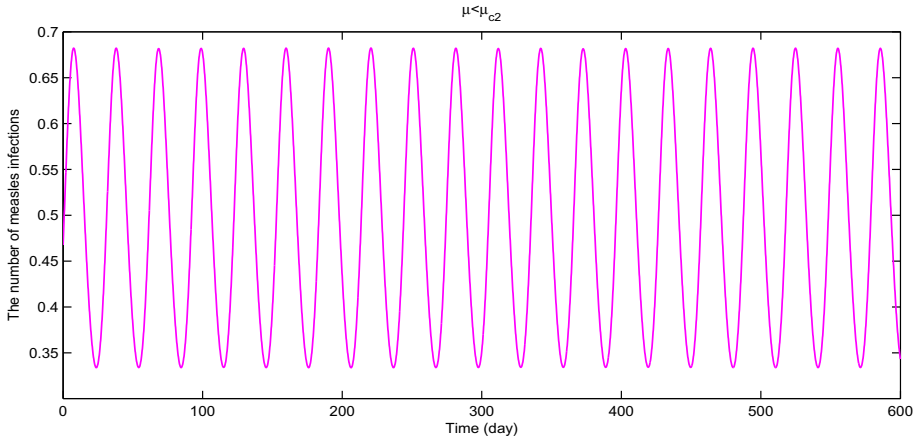

Fig. 5. The plot represents the oscillation of the number of infectious individuals $I(t)$ with time when $\mu = 0.2$ ($\mu < \mu_{c2}$).

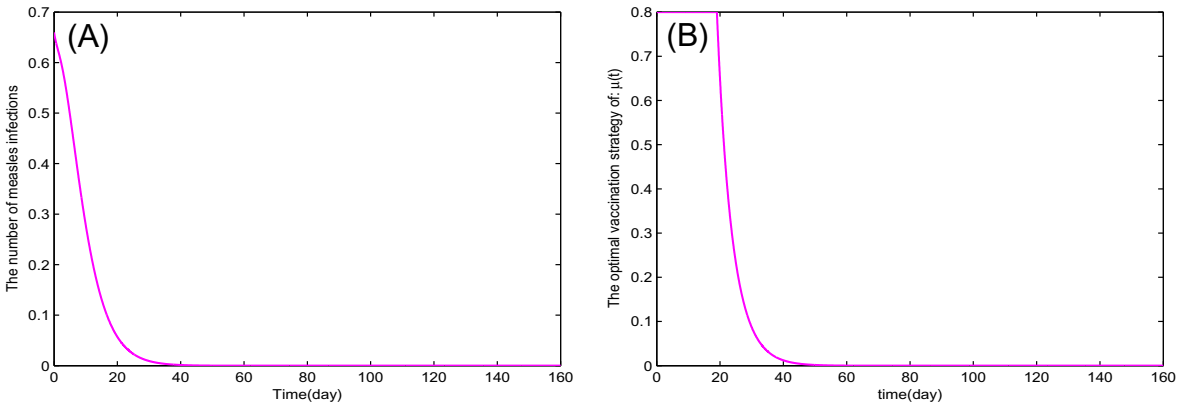

Fig. 6. (A) The change of the number of infectious individuals $I(t)$ under the optimal vaccination strategy $\mu^*(t)$ with time, and (B) the variation of optimal vaccination strategy $\mu^*(t)$ with time.

Table 1
The data of measles cases from 1951 to 1962 in U.S. (thousands).

Year	1951	1952	1953	1954	1955	1956	1957	1958	1959	1960	1961	1962
Cases	450	680	450	680	550	600	500	760	400	430	410	470

Case 5: Fitting the data of measles cases in the U.S. from 1951 to 1962.

To verify the reasonableness of our model, we simulate the data of measles cases in the U.S. from 1951 to 1962 by model (1.1). According to the report of CDC [10], the data of measles cases from 1951 to 1962 are given in Table 1. We fix the carrying capacity of the susceptible $\frac{1}{b} = 2.00 \times 10^{10}$, i.e., $b = 5.00 \times 10^{-11}$. Since the vaccine of measles was licensed in 1963, the vaccination ratio of the susceptible is equal to 0 before 1963 (i.e., $\mu = 0$). The initial values of the susceptible $S(0)$, exposed $E(0)$, infectious $I(0)$, the intrinsic growth rate r, the infective rate β, the natural death rate d, the rate of progression to infectious α and the recovered rate δ are regarded as parameters. We estimate those parameters by calculating the minimum sum of square (MSS) (Zhang et al. [41])

$$MSS = \sum (\log_2(\text{data per year}) - \log_2(\text{cases on the first month} + \cdots + \text{cases on the twelfth month}))^2$$

with Matlab tool fminsearch, which is part of the optimization of toolbox. All estimated values of those parameters are obtained as follows: $r = 16.1526$ per month, $\beta = 9.9514 \times 10^{-3}$ per month, $d = 2.0322 \times 10^{-3}$ per month, $\alpha = 1.6835$ per month and $\delta = 1.5772$ per month. The effect of fitting is exhibited in Fig. 7 which shows that the simulation provides a good match with the data of measles cases in the U.S. from 1951 to 1962.

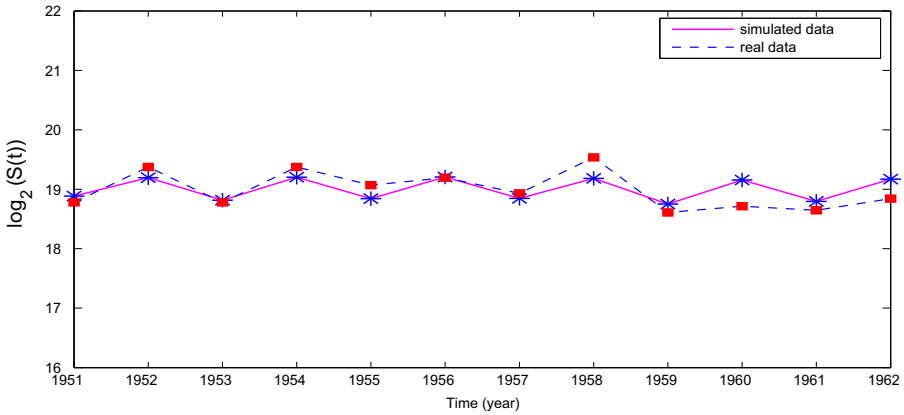

Fig. 7. Comparison of the reported measles data in the U.S. from 1951 to 1962 and the simulated solution $I(t)$ of model (1.1).

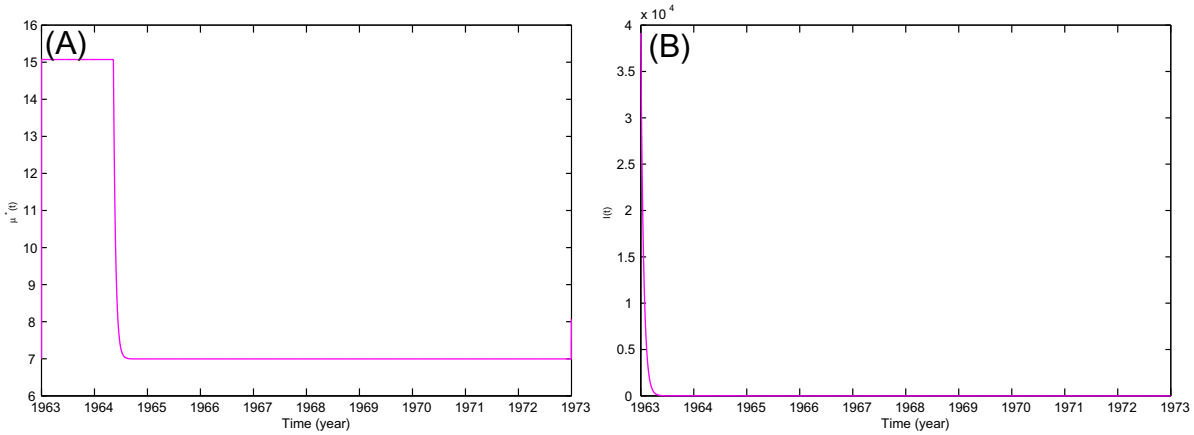

Fig. 8. (A) The variation of optimal vaccination strategy $\mu^*(t)$ with time and (B) the number of infectious individuals $I(t)$ under optimal vaccination strategy $\mu^*(t)$ with time.

Case 6: Optimal control strategy of US measles in the U.S.

According to the parameter values obtained from the real measles data in the U.S., we design a vaccination strategy to prevent the outbreak of measles in the U.S. Since vaccination for measles was licensed in 1963, we use the number of cases reported in December 1962 as the initial value of system (1.1), that is $I(0) = 4.7 \times 10^6/12 = 3.9167 \times 10^4$. In addition, we take the vaccination period $T = 120$ months (i.e. 10 years). In order to reduce errors, we adopt the sixth-order Runge–Kutta method to approximatively simulate the optimal control $\mu^*(t)$. The change of the vaccination coverage ratio $\mu^*(t)$ with time is shown in Fig. 8(A), and the number of infectious individuals $I(t)$ under the optimal vaccination strategy $\mu^*(t)$ with time is exhibited in Fig. 8(B). From Fig. 8, we know that adopting vaccination strategy $\mu^*(t)$ can effectively control the spread of measles in U.S. Hence, as proposed in [39], the partial-offset subsidy vaccination policy should be adopted between 1963 and 1965 and a voluntary vaccination policy can be taken after 1965.

7. Conclusion

Great attention has been paid to the investigation of the existence of complex dynamics, such as oscillations and chaos, in measles epidemic models (Bolker and Grenfell [7], Earn et al. [16], Grenfell [19]). It is believed and has been shown that such dynamics are strongly related to the seasonal forcing (Conlan and Grenfell [12]). In this paper, based on the mechanism and characteristics of measles transmission, we proposed a susceptible-exposed-infectious-recovered (SEIR) epidemic model with vaccination and studied the effect of vaccination in controlling the spread of measles. Two critical threshold values, μ_{c1} and μ_{c2}, of vaccine coverage ratio were obtained. It was shown that measles will be extinct when the vaccination ratio $\mu > \mu_{c1}$, will be endemic when $\mu_{c2} < \mu < \mu_{c1}$, and will be outbreak periodically when $\mu < \mu_{c2}$. Moreover, we applied the optimal control theory to obtain an optimal vaccination strategy $\mu^*(t)$ and gave some numerical simulations for those theoretical findings. Therefore, we were be able to prove the periodic outbreaks of measles in our model without the seasonal forcing.

Based on our model, its analysis, and the numerical simulations, we can provide some explanation on the characteristics of the measles epidemics in the United States from 1950 to 2009. Due to the absence of measles vaccination before 1963, about 500,000 measles cases and 500 deaths were reported annually, and with epidemic cycles every 2–3 years, which is in accord with our theoretical analysis. At this point, vaccine immunization rate μ is lower than μ_{c2}, and then the number of infectious individuals will exhibit periodical outbreaks. Following the licensure of vaccine in 1963, the incidence of measles declined more than 98%, and 2–3 year epidemic cycles no longer appeared, which indicates the number of measles cases was stabilized at a fixed value when the vaccination rate exceeds one critical threshold value μ_{c2} but it is less than the other critical threshold value μ_{c1}. Because measles vaccination ratio among 2-years-old children rose from 70% in 1990 to 91% in 1997, the reported cases descended rapidly after the 1989–1991 resurgence. This decline was due to a high vaccination ratio of preschool-aged children. Fewer than 500 cases have been reported annually since 1993, and fewer than 200 cases per year have been reported since 1997. A record of total 37 cases was reported in 2004. Measles elimination in the U.S. was achieved in 2004, which implies that as the vaccination ratio increases further, then the cases of measles infection reduce gradually, especially when the vaccination ratio is more than the larger critical value μ_{c1}, the measles is extinct. Hence, our model can illustrate the spread of measles in the United States reasonably and also verify the effectiveness of measles vaccination. In fact we fit the data of measles cases in the U.S. from 1951 to 1962.

The data on measles cases reported by the Chinese Center for Disease Control and Prevention (CCDC [11]) were presented in Fig. 1(B). We believe that the situation in China now is probably close to the case when the vaccination ratio $\mu > \mu_{c1}$. How to estimate parameters so that our model can be used to simulate the data in Fig. 1(B)? What effective control and prevention strategies should be implemented so that measles can be eradicated in China? We leave these for future consideration.

7.1. Acknowledgments

We would like to thank the two anonymous reviewers for their valuable comments and suggestions.

Appendix A

We discuss the stability and the direction of the bifurcating periodic solutions with the help of the normal form theory. First we transform the equilibrium $E^*(x^*, y^*, z^*)$ to the origin by the transformations

$$X = x - x^*, \quad Y = y - y^*, \quad Z = z - z^*,$$

under which, splitting off the linear part A_*H and the non-linear part B_* of model (2.1) yields

$$\dot{H} = A_*H + B_*, \tag{A.1}$$

where

$$H = \begin{bmatrix} X \\ Y \\ Z \end{bmatrix}, \quad A_* = \begin{bmatrix} -rx^* & 0 & -x^* \\ z^* & -\alpha_1 & x^* \\ 0 & \alpha_2 & -\alpha_3 \end{bmatrix}, \quad B_* = \begin{bmatrix} -rX^2 - XZ \\ XZ \\ 0 \end{bmatrix}.$$

By straightforward calculation, A_* has eigenvalues $\lambda_1 = -A_1, \lambda_2 = \omega i$ and $\lambda_3 = -\omega i$, whose eigenvectors can be expressed as

$$q_1 = \left[\frac{x^*}{\alpha_1+\alpha_3}, -\frac{rx^*+\alpha_1}{\alpha_2}, 1\right]^T, \quad q_2 = \left[-qrx^* + q\omega i, \frac{\alpha_3}{\alpha_2} + \frac{\omega}{\alpha_2} i, 1\right]^T, \quad q_3 = \left[-qrx^* - q\omega i, \frac{\alpha_3}{\alpha_2} - \frac{\omega}{\alpha_2} i, 1\right]^T,$$

where $q = \frac{1}{r(rx^*+\alpha_1+\alpha_3)}$.

Since

$$A_*[\mathrm{Im}(q_2), \mathrm{Re}(q_2), q_1] = [\omega \mathrm{Re}(q_2), -\omega \mathrm{Im}(q_2), \lambda_1 q_1] = [\mathrm{Im}(q_2), \mathrm{Re}(q_2), q_1] \begin{bmatrix} 0 & -\omega & 0 \\ \omega & 0 & 0 \\ 0 & 0 & \lambda_1 \end{bmatrix}, \tag{A.2}$$

we have

$$P = [\mathrm{Im}(q_2), \mathrm{Re}(q_2), q_1] = \begin{bmatrix} q\omega & -qrx^* & \frac{x^*}{\alpha_1+\alpha_3} \\ \frac{\omega}{\alpha_2} & \frac{\alpha_3}{\alpha_2} & -\frac{rx^*+\alpha_1}{\alpha_2} \\ 0 & 1 & 1 \end{bmatrix},$$

and then

$$P^{-1} = \begin{bmatrix} a_{11} & a_{21} & a_{31} \\ a_{12} & a_{22} & a_{32} \\ a_{13} & a_{23} & a_{33} \end{bmatrix},$$

where

$$a_{11}=\frac{(\alpha_1+\alpha_3)(\alpha_1+\alpha_3+rx^*)}{q\omega(\alpha_1+\alpha_3+2rx^*)(\alpha_1+\alpha_3)+x^*\omega},\quad a_{12}=\frac{-(\alpha_1+\alpha_3)}{q(\alpha_1+\alpha_3+2rx^*)(\alpha_1+\alpha_3)+x^*},\quad a_{13}=\frac{\alpha_1+\alpha_3}{q(\alpha_1+\alpha_3+2rx^*)(\alpha_1+\alpha_3)+x^*},$$
$$a_{21}=\frac{\alpha_2x^*[qr(\alpha_1+\alpha_3)+1]}{q\omega(\alpha_1+\alpha_3+2rx^*)(\alpha_1+\alpha_3)+x^*\omega},\quad a_{22}=\frac{q\alpha_2(\alpha_1+\alpha_3)}{q(\alpha_1+\alpha_3+2rx^*)(\alpha_1+\alpha_3)+x^*},\quad a_{23}=\frac{-q\alpha_2(\alpha_1+\alpha_3)}{q(\alpha_1+\alpha_3+2rx^*)(\alpha_1+\alpha_3)+x^*},$$
$$a_{31}=\frac{qrx^*(rx^*+\alpha_1)(\alpha_1+\alpha_3)-\alpha_3x^*}{q\omega(\alpha_1+\alpha_3+2rx^*)(\alpha_1+\alpha_3)+x^*\omega},\quad a_{32}=\frac{x^*+q(rx^*+\alpha_1)(\alpha_1+\alpha_3)}{q(\alpha_1+\alpha_3+2rx^*)(\alpha_1+\alpha_3)+x^*},\quad a_{33}=\frac{q\alpha_3(\alpha_1+\alpha_3)}{q\omega(\alpha_1+\alpha_3+2rx^*)(\alpha_1+\alpha_3)+x^*\omega}.$$

Furthermore,

$$P^{-1}A_*P=\begin{bmatrix}0&-\omega&0\\ \omega&0&0\\ 0&0&\lambda_1\end{bmatrix}.$$

To put model (2.1) into normal form, we make another linear transformation

$$\begin{bmatrix}X\\Y\\Z\end{bmatrix}=P\begin{bmatrix}X_1\\Y_1\\Z_1\end{bmatrix}\Longleftrightarrow\begin{bmatrix}X_1\\Y_1\\Z_1\end{bmatrix}=P^{-1}\begin{bmatrix}X\\Y\\Z\end{bmatrix}$$

to obtain

$$\begin{bmatrix}\dot X_1\\ \dot Y_1\\ \dot Z_1\end{bmatrix}=P^{-1}A_*P\begin{bmatrix}X_1\\Y_1\\Z_1\end{bmatrix}+\begin{bmatrix}g_1(X_1,Y_1,Z_1)\\ g_2(X_1,Y_1,Z_1)\\ g_3(X_1,Y_1,Z_1)\end{bmatrix}=\begin{bmatrix}0&-\omega&0\\ \omega&0&0\\ 0&0&\lambda_1\end{bmatrix}\begin{bmatrix}X_1\\Y_1\\Z_1\end{bmatrix}+\begin{bmatrix}g_1(X_1,Y_1,Z_1)\\ g_2(X_1,Y_1,Z_1)\\ g_3(X_1,Y_1,Z_1)\end{bmatrix},\tag{A.3}$$

where

$$g_1(X_1,Y_1,Z_1)=-ra_{11}\left(q\omega X_1-qrx^*Y_1+\frac{x^*}{\alpha_1+\alpha_3}Z_1\right)^2+(a_{21}-a_{11})\left(q\omega X_1-qrx^*Y_1+\frac{x^*}{\alpha_1+\alpha_3}Z_1\right)(Y_1+Z_1),$$
$$g_2(X_1,Y_1,Z_1)=-ra_{12}\left(q\omega X_1-qrx^*Y_1+\frac{x^*}{\alpha_1+\alpha_3}Z_1\right)^2+(a_{22}-a_{12})\left(q\omega X_1-qrx^*Y_1+\frac{x^*}{\alpha_1+\alpha_3}Z_1\right)(Y_1+Z_1),$$
$$g_3(X_1,Y_1,Z_1)=-ra_{13}\left(q\omega X_1-qrx^*Y_1+\frac{x^*}{\alpha_1+\alpha_3}Z_1\right)^2+(a_{23}-a_{13})\left(q\omega X_1-qrx^*Y_1+\frac{x^*}{\alpha_1+\alpha_3}Z_1\right)(Y_1+Z_1).$$

Selecting a center manifold

$$Z_1=h(X_1,Y_1)=AX_1^2+BX_1Y_1+CY_1^2+\cdots,$$

leads to

$$\begin{aligned}\dot Z_1&=2AX_1\dot X_1+BY_1\dot X_1+BX_1\dot Y_1+2CY_1\dot Y_1\cdots=(2AX_1+BY_1)\dot X_1+(BX_1+2CY_1)\dot Y_1+\cdots\\&=(2AX_1+BY_1)[-\omega Y_1+g_1(X_1,Y_1,Z_1)]+(BX_1+2CY_1)[\omega X_1+g_2(X_1,Y_1,Z_1)]+\cdots\\&=B\omega X_1^2+(2C\omega-2A\omega)X_1Y_1-B\omega Y_1^2\cdots\end{aligned}\tag{A.4}$$

It follows from (A.3) that

$$\dot Z_1=\lambda_1X_1+g_3(X_1,Y_1,Z_1)=\lambda_1(AX_1^2+BX_1Y_1+CY_1^2+\ldots)+g_3(X_1,Y_1,Z_1)=b_1X_1^2+b_2X_1Y_1+b_3Y_1^2+\cdots\tag{A.5}$$

where

$$b_1=A\lambda_1-ra_{13}q^2\omega^2,$$

$$b_2=B\lambda_1+2a_{13}q^2r^2\omega x^*+(a_{23}-a_{13})q\omega,$$

$$b_3=C\lambda_1-a_{13}q^2r^3(x^*)^2-(a_{23}-a_{13})qrx^*.$$

Combing (A.4) and (A.5), we obtain

$$\begin{cases}B\omega=A\lambda_1-ra_{13}q^2\omega^2,\\ 2C\omega-2A\omega=B\lambda_1+2a_{13}q^2r^2\omega x^*+(a_{23}-a_{13})q\omega,\\ -B\omega=C\lambda_1-a_{13}q^2r^3(x^*)^2-(a_{23}-a_{13})qrx^*,\end{cases}$$

which gives

$$\begin{cases} A = \frac{1}{(4\omega^2+\lambda_1^2)\lambda_1}\left[a_{13}rq^2\omega^2(2\omega^2+2(x^*)^2r^2+\lambda_1^2-2r\lambda_1x^*)-(a_{23}-a_{13})q\omega^2(2rx^*-\lambda_1)\right], \\ B = \frac{1}{(4\omega^2+\lambda_1^2)\omega}\left[a_{13}rq^2\omega^2(2(x^*)^2-2r\lambda_1x^*-2\omega^2)-(a_{23}-a_{13})q\omega^2(2rx^*-\lambda_1)\right], \\ C = \frac{\omega}{(4\omega^2+\lambda_1^2)\lambda_1}\left[a_{13}rq^2(2\omega^2(x^*)^2r^2+x^*r^2\lambda_1^2-2x^*r\lambda_1\omega^2-2\omega^4)+(a_{23}-a_{13})q(2rx^*\omega^2+rx^*\lambda_1^2-\lambda_1\omega^2)\right]. \end{cases}$$

Hence, the normal form of model (2.1) is given by

$$\begin{bmatrix}\dot{X}_1\\ \dot{Y}_1\end{bmatrix} = \begin{bmatrix}0 & -\omega\\ \omega & 0\end{bmatrix}\begin{bmatrix}X_1\\ Y_1\end{bmatrix} + \begin{bmatrix}g^{(1)}(X_1,Y_1)\\ g^{(2)}(X_1,Y_1)\end{bmatrix}, \tag{A.6}$$

where

$$\begin{aligned} g^{(1)}(X_1,Y_1) &= g_1\left(X_1,Y_1,AX_1^2+BX_1Y_1+CY_1^2\right)\\ &= \frac{x^*}{\alpha_1+\alpha_3}(a_{21}-a_{11}-ra_{11}\frac{x^*}{\alpha_1+\alpha_3})(AX_1^2+BX_1Y_1+CY_1^2)^2+qA\omega(a_{21}-a_{11}-2ra_{11}\frac{x^*}{\alpha_1+\alpha_3})X_1^3\\ &+\left[\left(\frac{x^*}{\alpha_1+\alpha_3}-qrx^*\right)(a_{21}-a_{11})+2a_{11}qx^*r^2\frac{x^*}{\alpha_1+\alpha_3}\right]CY_1^3\\ &+\left[2a_{11}rq\frac{x^*}{\alpha_1+\alpha_3}(rx^*A-B\omega)+(a_{21}-a_{11})\left(qB\omega-qrx^*A+\frac{x^*}{\alpha_1+\alpha_3}A\right)\right]X_1^2Y_1\\ &+\left[2a_{11}qr\frac{x^*}{\alpha_1+\alpha_3}(rx^*B-C\omega)+(a_{21}-a_{11})\left(qC\omega+\frac{x^*}{\alpha_1+\alpha_3}B-qrx^*B\right)\right]X_1Y_1^2-ra_{11}q^2\omega^2X_1^2-[a_{11}q^2r^2x^*\\ &+(a_{21}-a_{11})qrx^*]Y_1^2+[2a_{11}q^2r^2x^*\omega+q\omega(a_{21}-a_{11})]X_1Y_1, \end{aligned}$$

$$\begin{aligned} g^{(2)}(X_1,Y_1) &= g_2\left(X_1,Y_1,AX_1^2+BX_1Y_1+CY_1^2\right)\\ &= \frac{x^*}{\alpha_1+\alpha_3}\left(a_{22}-a_{12}-ra_{12}\frac{x^*}{\alpha_1+\alpha_3}\right)\left(AX_1^2+BX_1Y_1+CY_1^2\right)^2+qA\omega\left(a_{22}-a_{12}-2ra_{12}\frac{x^*}{\alpha_1+\alpha_3}\right)X_1^3\\ &+\left[\left(\frac{x^*}{\alpha_1+\alpha_3}-qrx^*\right)(a_{22}-a_{12})+2a_{12}qx^*r^2\frac{x^*}{\alpha_1+\alpha_3}\right]CY_1^3\\ &+\left[2a_{12}rq\frac{x^*}{\alpha_1+\alpha_3}(rx^*A-B\omega)+(a_{22}-a_{12})\left(qB\omega-qrx^*A+\frac{x^*}{\alpha_1+\alpha_3}A\right)\right]X_1^2Y_1\\ &+\left[2a_{12}qr\frac{x^*}{\alpha_1+\alpha_3}(rx^*B-C\omega)+(a_{22}-a_{12})\left(qC\omega+\frac{x^*}{\alpha_1+\alpha_3}B-qrx^*B\right)\right]X_1Y_1^2-ra_{12}q^2\omega^2X_1^2\\ &-[a_{12}q^2r^2x^*+(a_{22}-a_{12})qrx^*]Y_1^2+[2a_{12}q^2r^2x^*\omega+q\omega(a_{22}-a_{12})]X_1Y_1. \end{aligned}$$

By using the formula in Hassard et al. [20] and Zhang and Chen [40] and complex calculations, we obtain the stability coefficient

$$\begin{aligned} K = K(0,0) &= \frac{1}{16}\left[\frac{\partial^3g^{(1)}}{\partial X_1^3}+\frac{\partial^3g^{(1)}}{\partial X_1\partial Y_1^2}+\frac{\partial^3g^{(2)}}{\partial X_1^2\partial Y_1}+\frac{\partial^3g^{(2)}}{\partial Y_1^3}\right]\\ &+\frac{1}{16\omega}\left[\frac{\partial^2g^{(1)}}{\partial X_1\partial Y_1}\left(\frac{\partial^2g^{(1)}}{\partial X_1^2}+\frac{\partial^2g^{(1)}}{\partial Y_1^2}\right)-\frac{\partial^2g^{(2)}}{\partial X_1\partial Y_1}\left(\frac{\partial^2g^{(2)}}{\partial X_1^2}+\frac{\partial^2g^{(2)}}{\partial Y_1^2}\right)-\frac{\partial^2g^{(1)}}{\partial X_1^2}\frac{\partial^2g^{(2)}}{\partial X_1^2}+\frac{\partial^2g^{(1)}}{\partial X_1^2}\frac{\partial^2g^{(2)}}{\partial Y_1^2}\right]\\ &= \frac{1}{16}\left\{6qA\omega\left(a_{21}-a_{11}-2ra_{11}\frac{x^*}{\alpha_1+\alpha_3}\right)+\left[4a_{11}qr\frac{x^*}{\alpha_1+\alpha_3}(rx^*B-C\omega)+(a_{21}-a_{11})\left(qC\omega+\frac{x^*}{\alpha_1+\alpha_3}B-qrx^*B\right)\right]\right.\\ &+\left[4a_{12}qr\frac{x^*}{\alpha_1+\alpha_3}(rx^*A-B\omega)+(a_{22}-a_{12})\left(qB\omega+\frac{x^*}{\alpha_1+\alpha_3}A-qrx^*A\right)\right]\\ &\left.+6C\left[2a_{12}qr^2x^*\frac{x^*}{\alpha_1+\alpha_3}+(a_{22}-a_{12})(\frac{x^*}{\alpha_1+\alpha_3}-qrx^*)\right]\right\}+\frac{1}{16\omega}\left\{[2a_{11}q^2r^2x^*\omega+q\omega(a_{21}-a_{11})]\right.\\ &\times[-2ra_{11}q^2\omega_2^2+2a_{11}q^2r^2x^*+2(a_{21}-a_{11})qrx^*]-[2a_{12}q^2r^2x^*\omega+q\omega(a_{22}-a_{12})]\\ &\times[-2ra_{12}q^2\omega^2+2a_{12}q^2r^2x^*+2(a_{22}-a_{12})qrx^*]-4a_{11}a_{12}r^2q^4\omega^4\\ &\left.+4[a_{12}q^2r^2x^*+(a_{22}-a_{12})qrx^*][a_{11}q^2r^2x^*+(a_{21}-a_{11})qrx^*]\right\}. \end{aligned}$$

Therefore, we have the following conclusion:

Proposition A.1. *If Eq. (3.1) has a negative eigenvalue together with two purely imaginary eigenvalues, and the eigenvalues cross the imaginary axis with nonzero speed (i.e., $V_c = Re(\frac{d\lambda}{d\rho}|_{\rho=0}) \neq 0$), then the periodic orbits which are bifurcated from the equilibrium E^* are stable when $K < 0$ and unstable when $K > 0$. The direction of bifurcation are super-critical (sub-critical) when $V_c K < 0$ ($V_c K > 0$).*

We will give an example to investigate the stability of periodic solutions generated from the Hopf bifurcation.

Example A.2. Consider

$$\begin{cases} \dot{x} = rx(1-x) - xz - 0.4x, \\ \dot{y} = xz - 0.2z, \\ \dot{z} = 0.6y - 0.2z. \end{cases} \tag{A.7}$$

According to the above analyses, it is easy to see that if $0.4 < r < 0.4286$ (i.e., $\mathcal{R}_0 < 1$), then the disease-free equilibrium E_1 is globally asymptotically stable; if the $0.4286 < r < 0.6261$ or $r > 14.3739$ (i.e., $\mathcal{R}_1 < 1 < \mathcal{R}_0$), the endemic equilibrium E^* is asymptotically stable; if the $0.6261 < r < 14.3739$ (i.e., $\mathcal{R}_1 > 1$), the endemic equilibrium E^* is unstable. Especially, if $r = r_{c1} = 0.6261$ or $r = r_{c2} = 14.3739$, then the Jacobian matrix of model (A.7) at the endemic equilibrium E^* has a negative eigenvalue together with two purely imaginary eigenvalues, and the eigenvalues cross the imaginary axis with nonzero speed since $\mathrm{Re}(\frac{d\lambda}{d\rho}|_{r=r_{c1}}) = 0.0222 > 0$ and $\mathrm{Re}(\frac{d\lambda}{d\rho}|_{r=r_{c2}}) = -0.1062 < 0$. Hence, we can see that a Hopf bifurcation is bifurcated from the endemic equilibrium E^*. Next, we justify the stability and the direction of periodic solutions bifurcated from the endemic equilibrium E^*.

We only discuss the case for $r = r_{c1}$. From (A.6), the normal form of the model (A.7) is

$$\begin{bmatrix} \dot{X}_1 \\ \dot{Y}_1 \end{bmatrix} = \begin{bmatrix} 0 & -0.1292 \\ 0.1292 & 0 \end{bmatrix} \begin{bmatrix} X_1 \\ Y_1 \end{bmatrix} + \begin{bmatrix} g^{(1)}(X_1, Y_1) \\ g^{(2)}(X_1, Y_1) \end{bmatrix}, \tag{A.8}$$

where

$$\begin{aligned} g^{(1)} &= -0.2063X_1^2 + 0.1080Y_1^2 - 0.2678X_1Y_1 - 0.1334X_1^3 + 0.7204X_1^2Y_1 - 0.0903X_1Y_1^2 + 0.0029Y_1^3 - 0.0100X_1^4 \\ &\quad - 0.2926X_1^2Y_1^2 - 0.0012Y_1^4 + 0.1070X_1^3Y_1 + 0.0370Y_1^4, \\ g^{(2)} &= 0.0604X_1^2 - 0.2049Y_1^2 + 0.6149X_1Y_1 + 0.1696X_1^3 - 0.9032X_1^2Y_1 + 0.0480X_1Y_1^2 + 0.0007Y_1^3 + 0.0143X_1^4 \\ &\quad + 0.4164X_1^2Y_1^2 + 0.0017Y_1^4 - 0.1523X_1^3Y_1 - 0.0526Y_1^4. \end{aligned}$$

The coefficient of the stability is

$$\begin{aligned} K &= \frac{1}{16}(-0.1334 \times 6 - 2 \times 0.9032 - 2 \times 0.0903 + 6 \times 0.0007) + \frac{1}{16 \times 0.1292} \times [-2 \times 0.2678(-0.2063 + 0.1080) \\ &\quad - 2 \times 0.6149(0.0604 - 0.2049) + 4 \times 0.2063 \times 0.0604 - 4 \times 0.1080 \times 0.2049] = -0.0812 < 0. \end{aligned}$$

It follows from $\mathrm{Re}(\frac{d\lambda}{d\rho}|_{r=r_{c1}}) > 0$ and $K < 0$ that stable periodic orbits are bifurcated from the endemic equilibrium E^* and the direction of bifurcation is super-critical.

References

[1] R.M. Anderson, R.M. May, Infectious Diseases of Humans Dynamics and Control, Oxford University Press, Oxford, 1991.
[2] M.S. Bartlett, Measles periodicity and community size, J. R. Stat. Soc. A 120 (1957) 48–70.
[3] M.S. Bartlett, The critical community size for measles in the U.S., J R. Stat. Soc. A 123 (1960) 37–44.
[4] C.T. Bauch, D.J.D. Earn, Vaccination and the theory of games, Proc. Natl Acad. Sci. USA 101 (2004) 13391–13394.
[5] C.T. Bauch, A.P. Galvani, D.J.D. Earn, Group interest versus self-interest in smallpox vaccination policy, Proc. Natl Acad. Sci. USA 100 (2003) 10564–10567.
[6] S. Boccaletti, G. Bianconi, R. Criado, et al, The structure and dynamics of multilayer networks, Phys. Rep. 554 (2014) 1–122.
[7] B.M. Bolker, B.T. Grenfell, Chaos and biological complexity in measles dynamics, Proc. R. Soc. London B 251 (1993) 75–81.
[8] B.M. Bolker, B.T. Grenfell, Space, persistence and dynamics of measles epidemics, Philos Trans. R. Soc. Lond. B 348 (1995) 309–320.
[9] B.M. Bolker, B.T. Grenfell, Impact of vaccination on the spatial correlation and persistence of measles dynamics, Proc. Natl Acad. Sci. USA 93 (1996) 12648–12653.
[10] Centers for Disease Control and Prevention, Vaccines and Immunizations-Measles Epidemiology and Prevention of Vaccine-Preventable Diseases. <http://www.cdc.gov/vaccines/pubs/pinkbook/meas.html>.
[11] Chinese Center for Disease Control and Prevention, Measles. http://www.phsciencedata.cn/Share/ky_sjml.jsp?id=f17e302d-b0ef-4573-ae43-4fa55e7de9f5.
[12] A.J.K. Conlan, B.T. Grenfell, Seasonality and the persistence and invasion of measles, Proc. R. Soc. B 274 (2007) 1133–1141.
[13] R.V. Culshaw, S. Ruan, R.J. Spiteri, Optimal HIV treatment by maximising immune response, J. Math. Biol. 48 (2004) 545–562.
[14] O. Diekmann, J.A.P. Heesterbeek, Mathematical Epidemiology of Infective Diseases: Model Building, Analysis and Interpretation, Wiley, New York, 2000.
[15] O. Diekmann, J.A.P. Heesterbeek, M.G. Roberts, The construction of next generation matrices for compartmental epidemic models, J. R. Soc. Interface 7 (2000) 873–885.
[16] D.J.D. Earn, P. Rohani, B.M. Bolker, B.T. Grenfell, A simple model for complex dynamical transitions in epidemics, Science 287 (2000) 667–670.
[17] M.J. Ferrari, R.F. Grais, N. Bharti, A.J.K. Conlan, O.N. Bjrnstad, L.J. Wolfson, P.J. Guerin, A. Djibo, B.T. Grenfell, The dynamics of measles in sub-Saharan Africa, Nature 451 (2008) 679–684.

[18] W.H. Fleming, R.W. Rishel, Deterministic and Stochastic Optimal Control, Springer-Verlag, New York/Berlin, 1975.
[19] B.T. Grenfell, Chance and chaos in measles dynamics, J. R. Stat. Soc. B 54 (1992) 383–398.
[20] B.D. Hassard, N.D. Kazarinoff, Y.-H. Wan, Theory and Applications of Hopf Bifurcation, Cambridge University Press, Cambridge, 1981.
[21] T.K. Kar, A. Batabyal, Stability analysis and optimal control of an SIR epidemic model with vaccination, BioSystems 104 (2011) 127–135.
[22] J. Karrakchou, M. Rachik, S. Gourari, Optimal control and infectiology: application to an HIV/AIDS model, Appl. Math. Comput. 177 (2006) 807–818.
[23] M.J. Keeling, B.T. Grenfell, Disease extinction and community size: modeling the persistence of measles, Science 275 (1997) 65–67.
[24] M.J. Keeling, P. Rohani, Modeling Infectious Diseases in Humans and Animals, Princeton University Press, Princeton, NJ, 2007.
[25] D.E. Kirschner, S. Lenhart, S. Serbin, Optimal control of the chemotherapy of HIV, J. Math. Biol. 35 (1997) 775–792.
[26] S. Lenhart, J.T. Workman, Optimal Control Applied to Biological Models, Chapman Hall/CRC, Boca Raton, FL, 2007.
[27] D. Liu, S. Ruan, D. Zhu, Stable periodic oscillations in a two-stage cancer model of tumor and immune system interactions, Math. Biosci. Eng. 9 (2012) 347–368.
[28] P.L. Panum, Observations Made During the Epidemic of Measles on the Faroe Islands in the Year 1846, Delta Omega Society, Cleveland, 1940.
[29] P. van den Driessche, J. Watmough, Reproduction numbers and sub-threshold endemic equilibria for compartmental models of disease transmission, Math. Biosci. 285 (2002) 29–48.
[30] J. Wang, S. Liu, B. Zheng, Y. Takeuchi, Qualitative and bifurcation analysis using an SIR model with a saturated treatment function, Math. Comput. Model. 55 (2012) 710–722.
[31] L. Wang, X. Li, Spatial epidemiology of net worked metapopulation: an overview, Chin. Sci. Bull. 59 (2014) 3511–3522.
[32] L. Wang, Z. Wang, Y. Zhang, X. Li, How human location-specific contact patterns impact spatial transmission between populations?, Sci Rep. 3 (2013) 1468.
[33] World Health Organization, Measles, WHO Fact sheet No. 286, Updated February 2014. <http://www.who.int/mediacentre/factsheets/fs286/en/>.
[34] J. Zhang, The Geometric Theory and Bifurcation Problem of Ordinary Differential Equations, Peking University Press, Beijing, 1987.
[35] G. Zhang, Q. Sun, et al, Noise-induced enhancement of network reciprocity in social dilemmas, Chaos, Solitons Fractals 51 (2003) 31–35.
[36] H. Zhang, Z. Yang, Z. Wu, et al, Braess's paradox in epidemic game: better condition results in less payoff, Sci. Rep. 3 (2013) 3292.
[37] H. Zhang, J. Zhang, C. Zhou, et al, Hub nodes inhibit the outbreak of epidemic under voluntary vaccination, New J. Phys. 12 (2010) 023015.
[38] H. Zhang, Z. Wu, M. Tang, Y. Lai, Effects of behavioral response and vaccination policy on epidemic spreading – an approach based on evolutionary-game dynamics, Sci. Rep. 4 (2014) 5666.
[39] H. Zhang, Z. Wu, X. Xu, et al, Impacts of subsidy policies on vaccination decisions in contact networks, Phys. Rev. E 88 (2013) 012813.
[40] X. Zhang, L. Chen, The periodic solution of a class of epidemic models, Comput. Math. Appl. 38 (1999) 61–71.
[41] X. Zhang, Y. Zhao, A. Neumann, Partial immunity and vaccination for influenza, J. Comput. Biol. 17 (2009) 1689–1696.
[42] C. Xia, Z. Wang, J. Sanz, et al, Effects of delayed recovery and nonuniform transmission on the spreading of diseases in complex networks, Physica A 392 (2013) 1577–1585.